Institut Pasteur
Microbes and Infection 14 (2012) 959–967
www.elsevier.com/locate/micinf

Original article

Infection of human THP-1 cells with dormant *Mycobacterium tuberculosis*

Elisabetta Iona [a,b], Manuela Pardini [a], Maria Cristina Gagliardi [a], Marisa Colone [c], Anna Rita Stringaro [c], Raffaela Teloni [a], Lara Brunori [a], Roberto Nisini [a], Lanfranco Fattorini [a], Federico Giannoni [a,*]

[a] *Dipartimento di Malattie Infettive, Parassitarie e Immunomediate, Istituto Superiore di Sanità, Viale Regina Elena, 299, 00161 Rome, Italy*
[b] *Centro Nazionale per la Ricerca e il Controllo dei Prodotti Immunobiologici, Istituto Superiore di Sanità, Viale Regina Elena, 299, 00161 Rome, Italy*
[c] *Dipartimento di Tecnologie e Salute, Istituto Superiore di Sanità, Viale Regina Elena, 299, 00161 Rome, Italy*

Received 21 November 2011; accepted 3 April 2012
Available online 14 April 2012

Abstract

Dormant, non-replicating *Mycobacterium tuberculosis* H37Rv strain cultured in hypoxic conditions was used to infect THP-1 cells. CFUs counting, Kinyoun staining and electron microscopy showed that dormant bacilli infected THP-1 cells at a rate similar to replicating *M. tuberculosis*, but failed to grow during the first 6 days of infection. The absence of growth was specific to the intracellular compartment, as demonstrated by efficient growth in liquid medium. Quantification of β-actin mRNA recovered from infected cells showed that, in contrast with log-phase bacteria, infection with dormant bacilli determined a reduced THP-1 cell death. Gene expression of intracellular non-replicating bacteria showed a pattern typical of a dormant state. Intracellular dormant bacteria induced the activation of genes associated to a proinflammatory response in THP-1 cells. Though, higher levels of TNFα, IL-1β and IL-8 mRNAs compared to aerobic H37Rv infected cells were not paralleled by increased cytokine accumulation in the supernatants. Moreover, dormant bacilli induced a higher expression of inducible cox-2 gene, accompanied by increased PGE2 secretion. Overall, our data describe a new model of *in vitro* infection using dormant *M. tuberculosis* that could provide the basis for understanding how non-replicating bacilli survive intracellularly and influence the maintenance of the hypoxic granuloma.

Keywords: *Mycobacterium tuberculosis*; Infection; PGE2

1. Introduction

The World Health Organization estimates that approximately one third of human population is latently infected with *Mycobacterium tuberculosis* (Mtb), making latent tuberculosis (TB) a virtually unlimited reservoir of bacilli surviving in an immunocompetent host. When the immune system wanes, as it may happen in people who suffer malnutrition, disease, or become old, post-primary active TB may develop. It is assumed that a substantial part of the 9 million of new TB cases diagnosed each year are due to reactivation of latent TB. During latent infection, Mtb is believed to survive in a non-replicating (dormant) state in which bacteria are mainly confined in hypoxic granulomatous lesions in the lung [1]. Dormant bacteria become more resistant to adverse conditions, survive high hypoxia [2] or nutrient deprivation [3], and are more tolerant to drugs [4–6]. Though, far from being a static condition, there is a general belief that during latent TB dormant Mtb enters limited stages of replication, infects new cells, colonizes new lung districts in a constant interplay between the attempts of Mtb to cause disease and the immune system trying to contain and eradicate infection [7].

Macrophages play a central role in defense against TB through phagocytosis, intracellular killing, antigen presentation to lymphocytes [8,9]. Upon infection of human acute monocytic leukemia THP-1 cells, a widely used model

* Corresponding author. Tel.: +39 06 49902318; fax: +39 06 49902886.
E-mail addresses: federico.giannoni@iss.it, giannoni@iss.it (F. Giannoni).

1286-4579/$ - see front matter © 2012 Institut Pasteur. Published by Elsevier Masson SAS. All rights reserved.
doi:10.1016/j.micinf.2012.04.003

mimicking macrophage–Mtb interactions, the microorganism replicates intracellularly at a rate similar to that of extracellular bacteria [10]. Moreover, Mtb subcellular components such as the cell wall lipoarabinomannan trigger a cascade of proinflammatory cytokines and chemokines which upregulate key components of the host defense to Mtb [11,12].

From early infection to late TB stages, the granuloma undergoes a morphological evolution, in which the bacilli are intracellular at the beginning of infection and extracellular when the necrotic caseous lesion progresses [13]. In this dynamic scenario, reinfection of peripheral macrophages surrounding the granuloma can occur, with infecting Mtb being either replicating or dormant. In addition, intracellular logarithmically growing Mtb may become dormant inside macrophages, as hypoxia develops, making the interaction between the macrophage and dormant Mtb an interesting condition to be studied.

Some *in vitro* models to generate non-replicating Mtb have been developed and extensively characterized. Of these, the Wayne model is widely accepted as a landmark in the field [2]. It consists in culturing Mtb in sealed tubes generating a gradual oxygen deprivation which lead to the generation of non-replicating bacilli, likely mimicking those present in the hypoxic environment of the granuloma. In this model, bacteria undergo different non-replicating stages, called NRP-1 (Non-Replicating Persistence-1) and NRP-2, each characterized by defined hypoxic conditions and a typical pattern of gene expression.

In this study, we infected the human macrophage-like THP-1 cells with aerobic logarithmically growing, or NRP-2 dormant, Mtb and monitored bacterial growth, THP-1 cell viability and gene expression. This approach provided new insight on the intracellular life of these two different physiologic stages of Mtb.

2. Materials and methods

2.1. Bacterial cultures

Mtb H37Rv (ATCC 27294) was used for all experiments. Aerobic bacteria were grown in agitation in Dubos tween–albumin (DTA) broth (Difco, Detroit, Michigan, USA) and collected at the mid-log phase ($OD_{600} = 0.4$). Hypoxic dormant bacilli were obtained in DTA broth in stirred (120 rpm) glass tubes with tightly closed caps incubated at 37 °C for 21–26 days as previously described [2,14]. Control tubes with 1.5 μg/ml final concentration of methylene blue as an indicator of oxygen depletion were added. Cultures were centrifuged at 1500 × g for 20 min, washed three times in RPMI 1640 medium (Euroclone ltd, Paignton, UK) and resuspended in RPMI containing 10% fetal bovine serum (FBS, Euroclone). Aliquots were stored at −80 °C until use. A few days after freezing, determination of the number of CFUs was carried out in Middlebrook 7H10 agar (Difco Laboratories, Detroit, Mi) plates incubated at 37 °C for 21 days in a humidified 5% CO_2 atmosphere.

2.2. Infections of THP-1 cells

The human monocytic cell line THP-1 was purchased from ATCC (TIB-202). THP-1 cells were cultured in RPMI 1640 supplemented with 10% FBS, 1 mM sodium pyruvate, 1% nonessential amino acids, 100 μg/ml kanamycin and 1% glutamine (Hyclone, Logan, UT), and incubated at 37 °C plus 5% CO_2. For infection experiments, 3×10^5 THP-1 cells/ml were passaged in complete RPMI containing 30 ng/ml phorbol myristate acetate (PMA, Sigma Chemical Co, St. Louis, MO) and plated for differentiation to macrophages. After 48 h, supernatants were removed and aerobic and dormant Mtb culture stocks were thawed and used to infect THP-1 cells at Multiplicity of Infection (MOI) of 5:1 (5 bacteria/1 cell) for 3 h. Cells were then washed 4 times with complete RPMI to remove extracellular bacilli. At various times, the infected cells were lysed in distilled water containing 0.1% saponin for 5 min at room temperature to determine the numbers of CFU/ml on Middlebrook 7H10 agar. In some experiments, infections were performed in CultureWell™ Chambered Coverglass plates (Molecular Probes, Inc., Eugene, Oregon, U.S.A.) using 5 μm membrane filtered Mtb to decrease the presence of bacterial clumps and a MOI of 2:1. Slides with infected cells were fixed with 10% formalin and intracellular mycobacteria were stained by the Kinyoun method.

2.3. Transmission electron microscopy

For ultrathin cryosections, cells were fixed with 4% paraformaldehyde plus 0.1% glutaraldehyde in PBS pH 7.4 (Euroclone) for 2 h, washed and embedded in 2% agarose low melting point that was solidified on ice. Agarose blocks were infused with sucrose 2.3 M overnight at 4 °C, frozen in liquid nitrogen, and cryosectioned following the Tokuyasu's method [15] using the Ultracut UCT device (Leica Microsystems, Wien, Austria). Ultrathin cryosections were collected using sucrose and methylcellulose and incubated with specific mAbs anti-LAMP-1 (Becton Dickinson, Sparks, Md) and anti-α-crystallin (IT-20, Colorado State University), then revealed with anti-Mouse IgG conjugates of different gold sizes (5 or 10 nm, as appropriate) (1:10 diluted; Sigma). Finally, ultrathin cryosections were stained with solutions of methylcellulose/uranyl acetate before electron microscopy examination. Observations were performed using the Philips 208 transmission electron microscope (FEI Company, Eindhoven, The Netherlands).

2.4. RNA extraction, reverse transcription and qReal-Time PCR

For THP-1 cells and intracellular Mtb total RNA extraction, supernatants were removed and cells were lysed directly in TRIzol reagent (Invitrogen, Carlsbad, CA, USA). Cell lysates were transferred into 1.5 ml screw cap tubes containing approximately 500 μl of 0.1 mm zirconia/silica beads (BioSpec Products Inc., Bartlesville, OK, USA) and centrifuged for 8 min at 6000 × g. Supernatants were recovered and processed for THP-1 total RNA extraction. The pellets containing

intracellular bacteria were resuspended in 1 ml of TRIzol reagent and passed through 6 cycles of 50 s each at maximum speed using a Mini-Beadbeater-8 (BioSpec Products Inc.). Both THP-1 and bacterial lysates were then additioned with chloroform and centrifuged. The upper phase was loaded on TRIzol Plus RNA purification kit columns (Invitrogen), following manufacturer's instructions. The RNA was eluted in 80 µl of H_2O and treated directly with 10 U RQ1 RNase-free DNase (Promega, Madison, WI, USA) at 37 °C for 1.5 h using the supplied buffer, before a new phenol–chloroform extraction and ethanol precipitation. From 1 to 2 µg, total RNA was resuspended in 4 µl of H_2O and 0.5 µg random hexamers were added up to a final volume of 5 µl, then RNA was heated at 70 °C for 5 min, chilled on ice and reverse transcribed in a final volume of 20 µl using 1 µl ImProm-II reverse transcriptase (Promega), in ImProm-II Reaction Buffer containing 0.5 mM dNTPs and 3 mM $MgCl_2$.

Quantitative Real-Time PCRs from THP-1 cDNA was performed in an iCycler iQ (Bio-Rad, Hercules, Calif.) with iQ SYBR Green Supermix (Bio-Rad) and 500 nM each primer for 40 cycles as follows: 40 s at 95 °C, 40 s at 57 °C, and 50 s at 72 °C for 40 cycles. When Mtb cDNA was used, the annealing temperature was 59 °C. A final melting curve was performed to analyze the product size and quality of the amplification. To determine the relative expression for each THP-1 and Mtb gene examined at different conditions and time points, the ΔCt was calculated by subtracting the β-actin or 16S threshold cycle (Ct) to the Ct obtained for each gene in each cDNA sample. Next, the ΔΔCt was calculated by subtracting the ΔCt for each condition to the ΔCt of uninfected THP-1 control cells at the end of the 3 h infection procedure. Finally, the fold change compared to THP-1 uninfected control was calculated using the formula $2^{-\Delta\Delta Ct}$. When Mtb cDNAs were used, ΔΔCt was calculated using intracellular log-phase bacteria at time zero post-infection as reference. All reactions were performed in triplicate and all RNAs were tested for the absence of genomic DNA contamination using non-reverse transcribed RNA for qPCR.

2.5. Determination of cell viability by qRT-PCR

3 µg XbaI linearized plasmid pSK-GFP (kindly provided by Dr. Furio Spano) was transcribed *in vitro* using 40 units of T7 RNA Polymerase (Promega) in a final volume of 100 µl, following the manufacturer's instructions. Uninfected and Mtb infected cells were lysed in TRIzol reagent containing synthetic GFP RNA (20 pg per condition). Total RNA was extracted and reverse transcribed as previously described. qPCR was performed using primers specific for GFP and human β-actin cDNAs. GFP RNA was used as normalizer to quantify β-actin mRNA, and the ΔCt and ΔΔCt were calculated as described below (Table 1).

2.6. Cytokine determination

Culture supernatants were collected at different times after THP-1 cell infection and frozen until use. IL-8, IL-1β and TNFα were measured by enzyme linked immunosorbent assay (ELISA) using commercially available kits (Endogen, Thermo Fisher Scientific Inc. Rockford, IL, USA). PGE2 was measured using a competitive ELISA kit from Cayman Chemical Co. (Ann Arbor, MI). The experimental protocols were as from the manufacturer's instructions, and cytokine levels were expressed in pg/ml. Detection limit of the assays was 15 pg/ml.

2.7. Statistical analysis

Statistical significance was determined by unpaired Student's *t* test.

3. Results

3.1. Mtb intracellular localization and growth

Fig. 1 (panels A–D) shows the microscopic appearance of THP-1 cells infected with log-phase or dormant Mtb after 3 h or 6 d post-infection. To avoid the presence of bacterial clumps and better appreciate late time point intracellular replication, Mtb containing medium was filtered prior infection with a 5 µm membrane. No major difference in the intracellular number of bacteria was observed after 3 h, demonstrating a similar capacity of the THP-1 cells to phagocytose log-phase or dormant Mtb. In contrast, at day 6, bacterial growth was much more evident for log-phase bacilli than for dormant bacilli. Using an equal number of log-phase

Table 1
Oligonucleotides used in qRT-PCR assays.

Gene	Forward	Reverse
β-actin	TCCTTCCTGGGCATGGAGTC	CAGGAGGAGCAATGATCTTGATC
IL-1β	CTAAACAGATGAAGTGCTCCTTCC	GAAAGAAGGTGCTCAGGTCATTC
IL-8	GGAACCATCTCACTGTGTGTAAAC	GGTCCACTCTCAATCACTCTCAG
TNFα	GCCTCTTCTCCTTCCTGATCG	CTTGAGGGTTTGCTACAACATGG
GFP	GGGAGACACCCTCGTCAACAGG	GTTGCACGCCGCCGTCTTC
16S	GCAGCAGTGGGGAATATTGCACAA	TCCACCTACCGTCAATCCGAGAGA
esat-6	CGCAATCCAGGGAAATGTCACGTC	GTACGCCTCCGAACCGCTACC
acr	CCGAGCGCACCGAGCAGAAG	GCCTTAATGTCGTCCTCGTCAGCA
sigmaB	ATCCGCCAGGCCATCACC	TCCTCATCGGTGGCTTCGC
sigmaE	GCCCAACCCCGAGCAGATC	CGTACCGTCCCGAGCTTCAC
devR	ACTGTGCCGCGATCTGT	TCCCTTGATGTCTTTGACGA

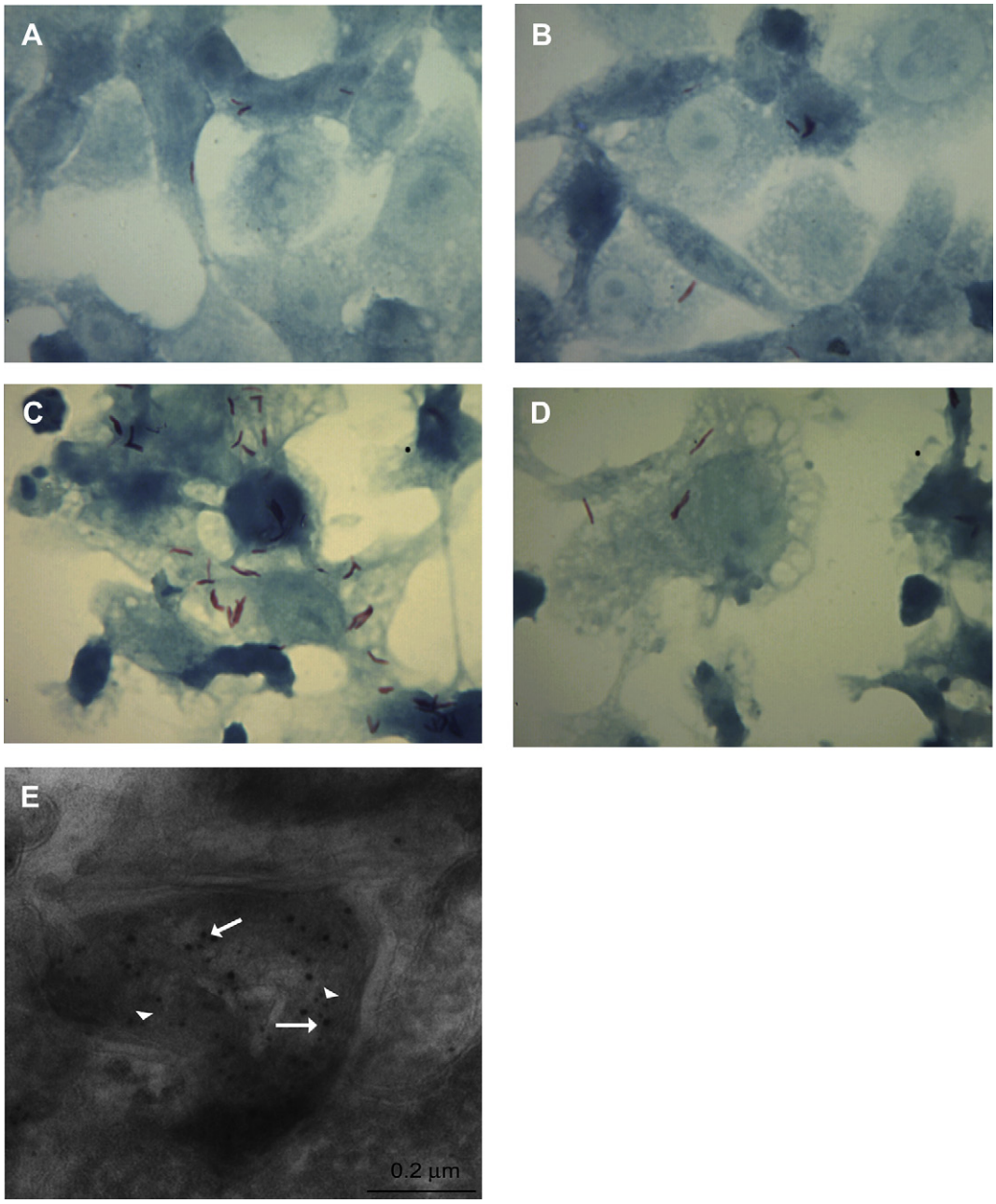

Fig. 1. Light and transmission electron microscopy of intracellular Mtb (A–D) stained with the Kinyoun method show THP-1 cells infected with aerobic (A–C) or dormant (B–D) Mtb at 3 h (A–B) and day 6 (C–D) post-infection. A MOI of 2:1 of 5 µm membrane filtered Mtb was used in this experiment. (E) Immunogold electron microscopy localization of Mtb from ultrathin cryosections of THP-1 cells infected with dormant Mtb, at 3 h after infection. Dormant intracellular Mtb was highly positive for α-crystallin (arrows) inside a Lamp-1 (arrowheads) positive vesicle.

and dormant bacilli for infection, not statistically different values of CFU/ml from THP-1 lysates were observed after 3 h of infection (4.56 ± 0.65 log10 CFU/ml for aerobic bacteria *versus* 4.23 ± 0.58 log10 CFU/ml for dormant bacteria, respectively) in four independent experiments. Since in our knowledge this is the first description of infection using dormant Mtb, we tested whether also non-replicating Mtb is phagocytosed and recovered intracellularly after infection. To investigate the intracellular localization of dormant Mtb, infected monolayers were processed for cryo-immunoelectron microscopy. Cryosections of infected THP-1 cells were double labeled for the expression of LAMP-1 and α-crystallin antigens. Fig. 1E shows that intracellular Mtb are highly positive for α-crystallin (large gold particles: arrows) both at the cell surface and inside the bacterial body. Mtb cells have been generally detected inside large vesicular structures (phagosomes) as revealed by the labeling with anti-LAMP-1 antibody (smaller particles: arrowheads).

Fig. 2 shows the intracellular and extracellular growth of aerobic and dormant Mtb compared to the growth in Middlebrook 7H9 medium. The number of intracellular dormant Mtb decreased from day 0 to day 6 while aerobic bacteria

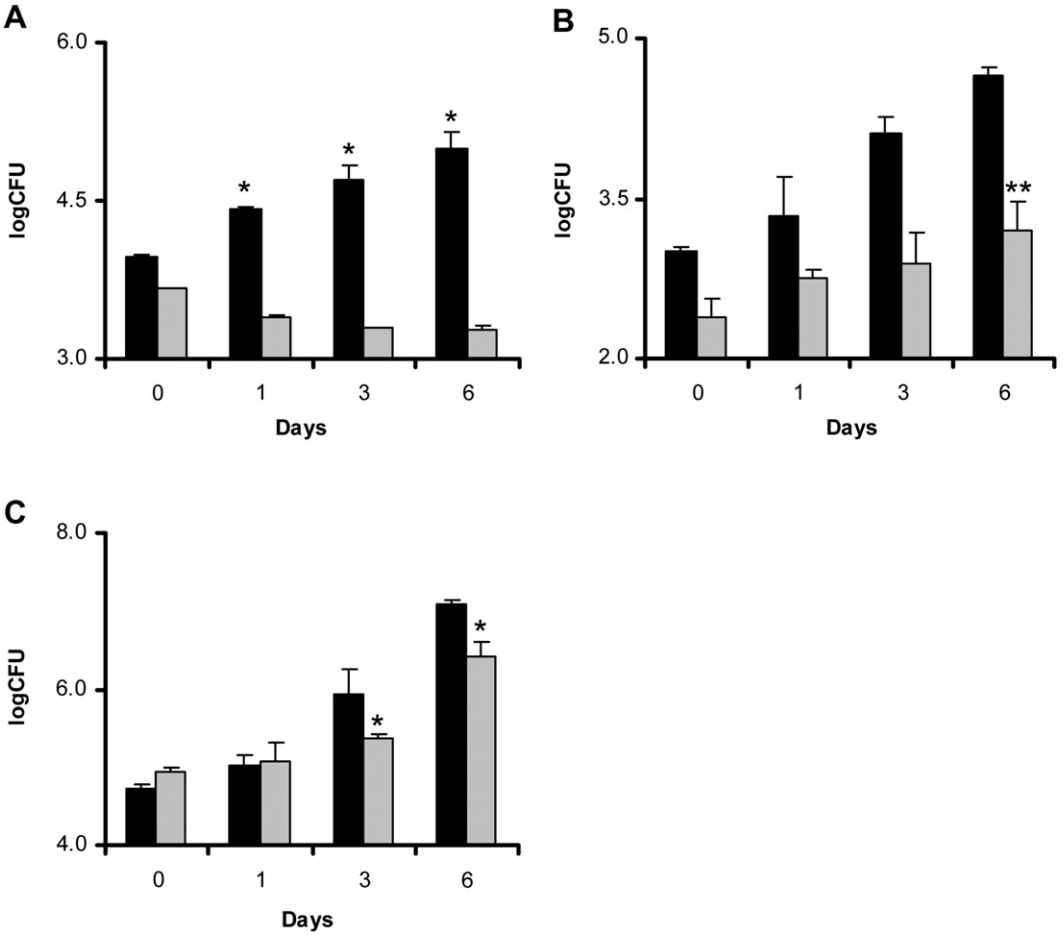

Fig. 2. Intracellular growth of log-phase and dormant Mtb. PMA-differentiated THP-1 cells were infected with log-phase Mtb (black bars) or dormant Mtb (gray bars). (A) THP-1 lysate; (B) THP-1 supernatants; (C) Middlebrook 7H9 broth. *$P < 0.001$ compared to time 0, **$P < 0.02$ compared to time 0.

increased about 10 times in the same period (Fig. 2A). This observation suggests that the intraphagosomal environment is able to keep dormant bacteria in a non-replicative stage at least up to day 6. A strong support to this hypothesis comes from the observation that both aerobic and dormant Mtb efficiently grew in the THP-1 supernatants (Fig. 2B) and in the 7H9 medium (Fig. 2C). Bacteria in cellular supernatants derive from unwashed Mtb as well as from host cell lysis.

3.2. Survival of THP-1 cells infected with replicating or dormant Mtb

Microscopic observation of THP-1 monolayers showed a much more rapid damage when log-phase bacteria were used for infection, compared to dormant bacilli. To this purpose, we measured the THP-1 cell viability by quantitating the amount of β-actin RNA extracted from uninfected, and aerobic or dormant Mtb infected THP-1 monolayers. As a housekeeping gene, the total amount of β-actin mRNA that can be recovered from THP-1 cells is directly proportional to the number of cells present. qRT-PCR specific for β-actin was performed and data were normalized using an internal control (GFP RNA) that was added to each sample at equal amounts at the time of cell lysis in TRIzol. GFP RNA was necessary for standardization among samples for differential RNA loss or degradation during extraction, or different efficiency during reverse transcription. Fig. 3A shows a decrease of total β-actin RNA recovered in control THP-1 monolayers at day 4 and 7 post-infection. This decrease was much more evident in cells infected with log-phase H37Rv, indicating detachment and lysis of adherent cells. In contrast, viability of dormant Mtb infected monolayers were fully preserved with time. Differences between β-actin mRNA recovered from monolayers and supernatants at day 4 and 7 post-infection were also examined (Fig. 3B). Cells infected with aerobic or dormant Mtb showed lower amounts of β-actin mRNA in the supernatants compared to monolayers, indicating that infected cells detaching from the plastic surface underwent rapid death. In contrast, control cells showed higher amounts of β-actin mRNA in the supernatants, suggesting a cell dedifferentiation process rather than death. This result strengthened the hypothesis that THP-1 cells limit the growth of non-replicating Mtb.

3.3. Mtb gene expression

Gene expression of intracellular log-phase and dormant Mtb was also determined (Fig. 4). In general, a higher

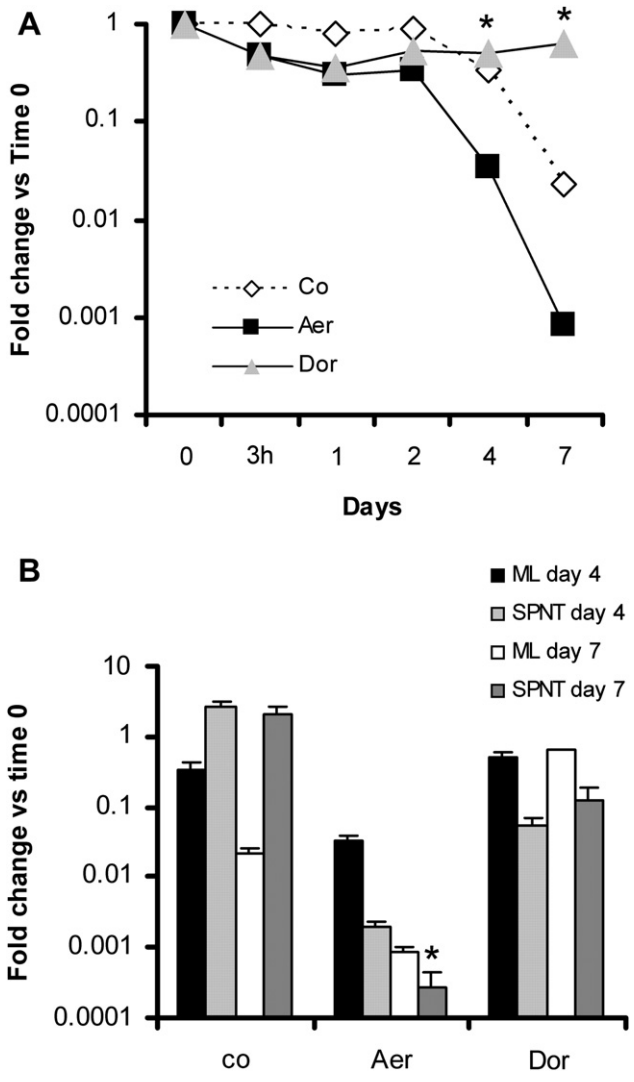

Fig. 3. THP-1 cell viability upon infection with log-phase (Aer) and dormant (Dor) Mtb. (A) total cellular RNA was extracted from monolayers of control and THP-1 cells infected with aerobic or dormant Mtb for 3 h (3 h) and incubated for 1, 2, 4 and 7 days. cDNA was synthesized and the amount of β-actin mRNA recovered was determined by qRT-PCR, normalized using synthetic GFP cDNA as described in the text and expressed as fold change compared to the β-actin mRNA recovered at time 0. *$P < 0.001$ compared to aerobic Mtb infected cells at day 4 and both uninfected and aerobic Mtb infected cells at day 7. (B) comparison between the amount of β-actin mRNA extracted from cellular monolayers (ML) and supernatant (SPNT) from control (co), aerobic (Aer) and dormant (Dor) Mtb-infected THP-1 cells at day 4 and 7 post-infection. Data are expressed as fold change compared to time 0 non-infected cells and normalized using synthetic GFP cDNA. All differences between ML and SPNT values were highly significant ($P < 0.001$). *$P < 0.02$ compared to ML day 7.

expression of dormancy-related genes, such as *sigmaB*, *sigmaE*, *devR* and α-crystallin (*acr*) in intracellular dormant bacteria was observed (Fig. 4A and B), compared to aerobic bacteria. As expected, a lower expression of *esat-6*, typically associated with early log-phase, was seen in dormant Mtb (Fig. 4C). These findings support the hypothesis that intracellular NRP-2 phase bacilli are maintained in a dormant phenotype up to day 4.

3.4. Cytokine gene expression and secretion

The cytokine response to the two different growth phases was investigated. Mtb activated an early response in the host cell by upregulating proinflammatory cytokines (IL-1β and TNF-α) and chemokines (IL-8). Fig. 5 panels A, C, E show the gene expression of these cytokines as determined by qRT-PCR. THP-1 cells infected with dormant Mtb expressed higher levels of mRNA for IL1-β, TNFα, and IL-8 compared to both control cells and log-phase Mtb infected cells. Despite these results, we observed no increase in cytokine accumulation in the supernatants of dormant Mtb infected cells compared to log-phase Mtb infected cells (Fig. 5, panels B, D and F). Recently, a large amount of data has been gathered on the PGE2 role in protecting macrophages from necrosis, directing the cells toward a proapoptotic pathway. Given our observation of a differential cell death triggered by the two different physiological conditions of Mtb, we tested gene expression of cox-2 and the parallel PGE2 secretion. We found that the dormant phase induced higher cox-2 mRNA levels and PGE2 secretion than the log-phase bacilli (Fig. 5, panels G, H).

4. Discussion

In this study we tested a new *in vitro* model in which two different physiological stages of Mtb were used to infect a human macrophage-like cell line. Dormant bacteria were found to be all viable at late NRP-2 stage, and able to restore growth when reincubated in fresh medium with a starting doubling time higher than 24 h (data not shown). In previous studies, Wayne and Hayes demonstrated that initial replication of late NRP-2 bacteria was synchronous [2]. These observations support the hypothesis that during the 3 h of our infection procedure, bacteria that are being phagocytosed have not resumed replication yet and can still be considered dormant. It is known that NRP-2-like Mtb may live in the rabbit, where solid and caseous granuloma resembling those of humans are formed [1]. In these lesions highly hypoxic conditions are reached, and susceptibility to metronidazole, a drug for anaerobes, is induced. We reported that in the Wayne model metronidazole effectively kills dormant Mtb after 20 days of incubation, thus in late NRP-2 phase [16]. Moreover, the dormancy regulon is upregulated *in vivo* [17] and, more recently, a second wave of genes, belonging to the so-called Enduring Hypoxic Response was shown to be induced in hypoxic conditions subsequently to the dormancy regulon [18], suggesting a role of this response also *in vivo*.

The results of the present study indicate that there are key differences between infection with dormant and log-phase Mtb in THP-1 cells. First of all, we found that, unlike aerobic Mtb, dormant bacilli are better contained in a non-replicating condition within the phagosome, in contrast to aerobic bacteria, implying that the macrophage competence to suppress intracellular growth of Mtb is related to the bacterial physiologic state. These observations also suggest that within the granuloma, once hypoxic conditions are established, Mtb infection may be more easily controlled by activated

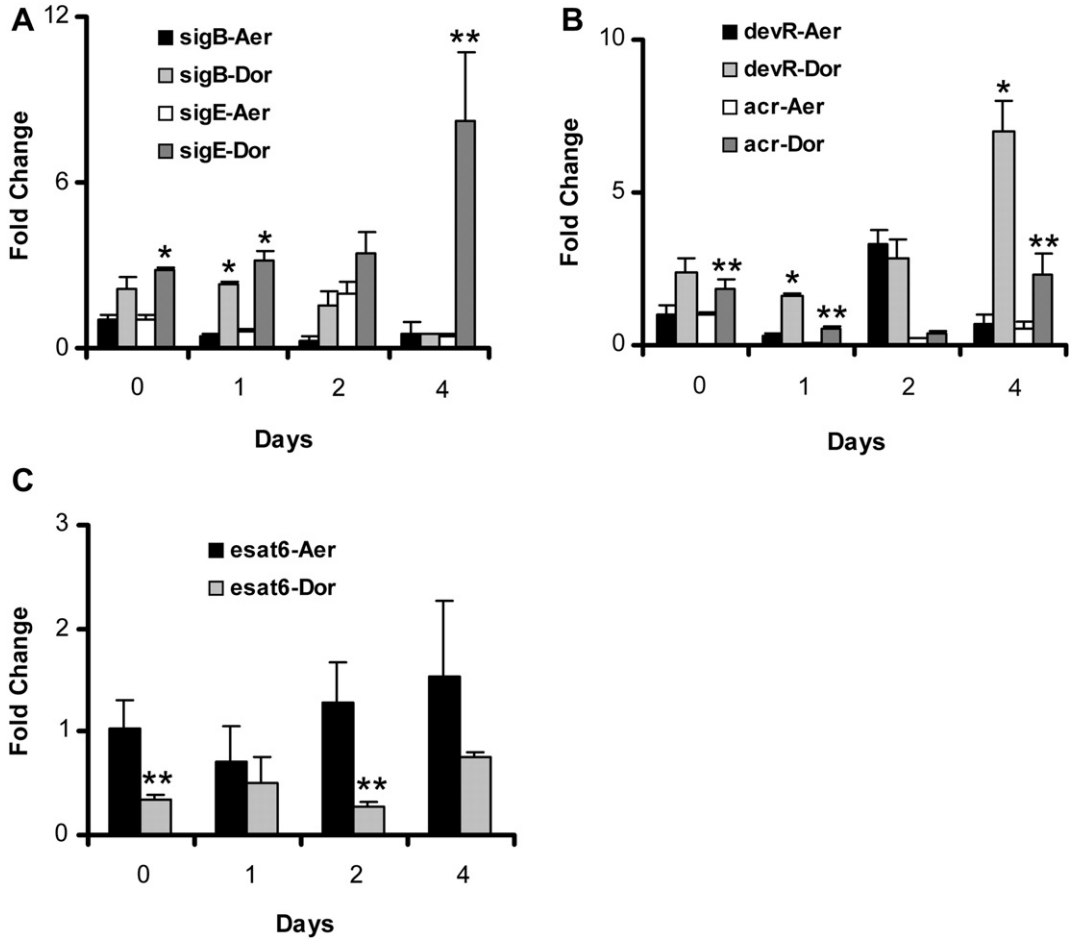

Fig. 4. Intracellular Mtb gene expression. Total Mtb RNA was extracted from infected THP-1 cells and qRT-PCR performed as described in materials and methods. Comparison of gene expression of intracellular log-phase (Aer) and dormant (Dor) Mtb is shown. (A) *sigmaB* and *sigmaE* genes, (B) *devR* and *acr* genes, (C) *esat-6* gene. *$P < 0.001$, **$P < 0.02$ compared to log-phase bacteria.

macrophages. Moreover, dormant bacteria showed a different gene expression pattern, compared to log-phase bacteria, with upregulation of dormancy-related genes (*acr*, *devR*, *sigmaB* and *sigmaE*) and down-regulation of genes more typical of the replicating form, such as *esat-6*, a well-known virulence factor which was demonstrated to be important in intracellular invasion and survival, with implications in the intracellular localization of Mtb [19,20].

The possibility that dormant Mtb may enter the host cell without inducing a strong cellular response, hiding undetected intracellularly, was not confirmed by our data. Indeed, we showed that the THP-1 cells responded very strongly to dormant Mtb. We observed differences in cytokine mRNA levels between the two physiologic forms, even if not paralleled by differential cytokine secretion. Recently, it has been shown that highly virulent strains of Mtb suppress cytokine gene expression compared to less virulent strains [21,22], suggesting that dormant Mtb may be detected by the macrophage as a less virulent form.

Furthermore, infection with the two different Mtb stages showed dramatic differences on cell viability. THP-1 cells infected with aerobic Mtb underwent cell lysis as bacteria started replication inside the cell, and at day 7 post-infection the cell monolayers were extensively damaged. By contrast, cells infected with dormant Mtb were quite stable over time and stayed even more attached to the flask than non-infected control cells. Clearly, the different ability of the two physiological forms to replicate and invade the cell plays a crucial role in this phenomenon. Though, other mechanisms could be involved. It has been demonstrated that macrophages infected by virulent Mtb undergo necrosis, whereas those infected by avirulent strains preferentially undergo apoptosis [23–26]. Recent studies reported a crucial role for the eicosanoids PGE2 and lipoxin (LX)A_4 in regulating cell death during mycobacterial infection [27,28]. In particular avirulent Mtb strains produce PGE2 that counteracts cell necrosis by protecting the mitochondrial inner membrane and inducing the repair of plasma membrane in infected macrophages, thus promoting cell apoptosis [28]. In contrast, virulent Mtb induces the production of LXA_4 that causes cell necrosis by inhibiting cox-2 expression and PGE2 synthesis [28], the release of proapoptotic mediators by mitochondria, and caspase activation [29]. We found that dormant Mtb induced cox-2 gene expression paralleled by an increased secretion of PGE2, compared to log-phase bacteria. We speculate that the increased secretion of PGE2 by dormant Mtb infected cells

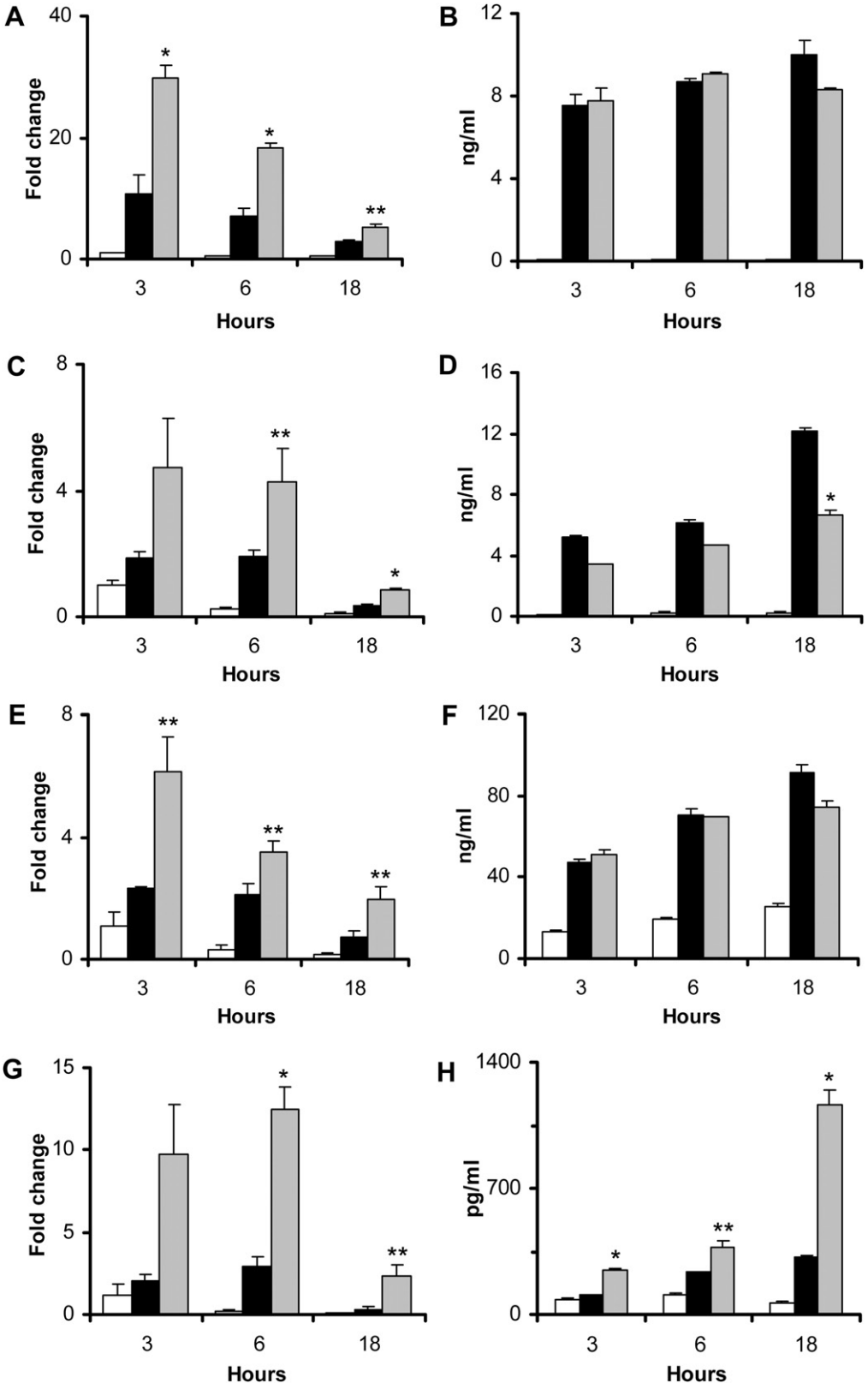

Fig. 5. THP-1 gene expression and secretion. PMA-differentiated THP-1 cells were infected with log-phase (black bars) or dormant (gray bars) Mtb. Infected THP-1 gene expression determined by qRT-PCR was compared to non-infected cells (white bars). Data are expressed as fold increase compared to 3 h post-infection non-infected cells. (A) TNF-α, (C) IL-1β, (E) IL-8, (G) cox-2. THP-1 secretion: (B) TNFα, (D) IL1β, (F) IL-8 and (H) PGE2 accumulation in the supernatants in control cells and after 3, 6 and 18 h infection of THP-1 cells with aerobic (black bars) and dormant Mtb (gray bars). A representative experiment out of three is shown. At 3 h post-infection, 5.06 log CFUs/ml in aerobic Mtb infected cells and 4.83 log CFUs/ml in dormant Mtb infected cells were counted at 3 h post-infection, confirming a comparable bacterial load in the two conditions. $*P < 0.001$, $**P < 0.02$, comparing log-phase and dormant Mtb infected cells.

may have an important role in host cell protection from necrosis. Future studies will be aimed to address this issue.

In conclusion, our data suggest a possible mechanism of hypoxic granuloma self renewing, in which dormant bacteria are much more easily controlled intracellularly and the structure of the granuloma is maintained by continuously recruiting new cells in response to the activity of macrophages infected with dormant *M. tuberculosis*.

Acknowledgments

This work was partially supported by the EC FP7 project StopLATENT-TB (grant agreement 200999) and by the EC FP7 NEWTBVAC project (grant agreement 241745). 16 kDa mouse monoclonal α-HspX antibody was received as part of NIH, NIAID Contract No. HHSN266200400091C, entitled "Tuberculosis Vaccine Testing and Research Materials" which was awarded to Colorado State University.

References

[1] L.E. Via, P.L. Lin, S.M. Ray, J. Carrillo, S.S. Allen, S.Y. Eum, K. Taylor, E. Klein, U. Manjunatha, J. Gonzales, E.G. Lee, S.K. Park, J.A. Raleigh, S.N. Cho, D.N. McMurray, J.L. Flynn, C.E. Barry 3rd, Tuberculous granulomas are hypoxic in guinea pigs, rabbits, and nonhuman primates, Infect. Immun. 76 (2008) 2333–2340.

[2] L.G. Wayne, L.G. Hayes, An *in vitro* model for sequential study of shiftdown of *Mycobacterium tuberculosis* through two stages of non-replicating persistence, Infect. Immun. 64 (1996) 2062–2069.

[3] T. Hampshire, S. Soneji, J. Bacon, B.W. James, J. Hinds, K. Laing, R.A. Stabler, P.D. Marsh, P.D. Butcher, Stationary phase gene expression of *Mycobacterium tuberculosis* following a progressive nutrient depletion: a model for persistent organisms, Tuberculosis 84 (2004) 228–238.

[4] J.E. Gomez, J.D. McKinney, *M. tuberculosis* persistence, latency, and drug tolerance, Tuberculosis 84 (2004) 29–44.

[5] Y. Zhang, Persistent and dormant tubercle bacilli and latent tuberculosis, Front. Biosci. 9 (2004) 1136–1156.

[6] S.H. Cho, S. Warit, B. Wan, C.H. Hwang, G.F. Pauli, S.G. Franzblau, Low-oxygen-recovery assay for high-throughput screening of compounds against nonreplicating *Mycobacterium tuberculosis*, Antimicrob. Agents Chemother. 51 (2007) 1380–1385.

[7] P.J. Cardona, A dynamic reinfection hypothesis of latent tuberculosis infection, Infection 37 (2009) 80–86.

[8] J. Pieters, *Mycobacterium tuberculosis* and the macrophage: maintaining a balance, Cell Host Microbe 3 (2008) 399–407.

[9] M.J. Fenton, M.W. Vermeulen, Immunopathology of tuberculosis: roles of macrophages and monocytes, Infect. Immun. 64 (1996) 683–690.

[10] S.A. Theus, M.D. Cave, K.D. Eisenach, Activated THP-1 cells: an attractive model for the assessment of intracellular growth rates of *Mycobacterium tuberculosis* isolates, Infect. Immun. 72 (2004) 1169–1173.

[11] Y. Zhang, M. Doerfler, T.C. Lee, B. Guillemin, W.N. Rom, Mechanisms of stimulation of interleukin-1 beta and tumor necrosis factor-alpha by *Mycobacterium tuberculosis* components, J. Clin. Invest. 91 (1993) 2076–2083.

[12] Y. Zhang, M. Broser, H. Cohen, M. Bodkin, K. Law, J. Reibman, W.N. Rom, Enhanced interleukin-8 release and gene expression in macrophages after exposure to *Mycobacterium tuberculosis* and its components, J. Clin. Invest. 95 (1995) 586–592.

[13] J. Grosset, *Mycobacterium tuberculosis* in the extracellular compartment: an underestimated adversary, Antimicrob. Agents Chemother. 47 (2003) 833–836.

[14] P. Filippini, E. Iona, G. Piccaro, P. Peyron, O. Neyrolles, L. Fattorini, Activity of drug combinations against dormant *Mycobacterium tuberculosis*, Antimicrob. Agents Chemother. 54 (2010) 2712–2715.

[15] K.T. Tokuyasu, A technique for ultracryotomy of cell suspensions and tissues, J. Cell. Biol. 57 (1973) 551–565.

[16] E. Iona, F. Giannoni, M. Pardini, L. Brunori, G. Orefici, L. Fattorini, Metronidazole plus rifampin sterilizes long-term dormant *Mycobacterium tuberculosis*, Antimicrob. Agents Chemother. 51 (2007) 1537–1540.

[17] L. Shi, Y.J. Jung, S. Tyagi, M.L. Gennaro, R.J. North, Expression of Th1-mediated immunity in mouse lungs induces a *Mycobacterium tuberculosis* transcription pattern characteristic of nonreplicating persistence, Proc. Natl. Acad. Sci. USA 100 (2003) 241–246.

[18] T.R. Rustad, M.I. Harrell, R. Liao, D.R. Sherman, The enduring hypoxic response of *Mycobacterium tuberculosis*, PLoS One 3 (2008) e1502.

[19] N. van der Wel, D. Hava, D. Houben, D. Fluitsma, M. van Zon, J. Pierson, M. Brenner, P.J. Peters, *M. tuberculosis* and *M. leprae* translocate from the phagolysosome to the cytosol in myeloid cells, Cell 129 (2007) 1287–1298.

[20] K.M. Guinn, M.J. Hickey, S.K. Mathur, K.L. Zakel, J.E. Grotzke, D.M. Lewinsohn, S. Smith, D.R. Sherman, Individual RD1-region genes are required for export of ESAT-6/CFP-10 and for virulence of *Mycobacterium tuberculosis*, Mol. Microbiol. 51 (2004) 359–370.

[21] K.C. Wong, W.M. Leong, H.K. Law, K.F. Ip, J.T. Lam, K.Y. Yuen, P.L. Ho, W.S. Tse, X.H. Weng, W.H. Zhang, S. Chen, W.C. Yam, Molecular characterization of clinical isolates of *Mycobacterium tuberculosis* and their association with phenotypic virulence in human macrophages, Clin. Vaccine Immunol. 14 (2007) 1279–1284.

[22] J.S. Kim, M.J. Ryu, E.H. Byun, W.S. Kim, J. Whang, K.N. Min, M. Shong, H.J. Kim, S.J. Shin, Differential immune response of adipocytes to virulent and attenuated *Mycobacterium tuberculosis*, Microbes Infect. 13 (2011) 1242–1251.

[23] J. Keane, H.G. Remold, H. Kornfeld, Virulent *Mycobacterium tuberculosis* strains evade apoptosis of infected alveolar macrophages, J. Immunol. 164 (2000) 2016–2020.

[24] M. Divangahi, M. Chen, H. Gan, D. Desjardins, T.T. Hickman, D.M. Lee, S. Fortune, S.M. Behar, H.G. Remold, *Mycobacterium tuberculosis* evades macrophage defenses by inhibiting plasma membrane repair, Nat. Immunol. 10 (2009) 899–906.

[25] S.M. Behar, C.J. Martin, M.G. Booty, T. Nishimura, X. Zhao, H.X. Gan, M. Divangahi, H.G. Remold, Apoptosis is an innate defense function of macrophages against *Mycobacterium tuberculosis*, Mucosal Immunol. 4 (3) (2011) 279–287 (Epub 2011 Feb 9).

[26] M. Chen, H. Gan, H.G. Remold, A mechanism of virulence: virulent *Mycobacterium tuberculosis* strain H37Rv, but not attenuated H37Ra, causes significant mitochondrial inner membrane disruption in macrophages leading to necrosis, J. Immunol. 176 (6) (2006) 3707–3716.

[27] M. Divangahi, D. Desjardins, C. Nunes-Alves, H.G. Remold, S.M. Behar, Eicosanoid pathways regulate adaptive immunity to *Mycobacterium tuberculosis*, Nat. Immunol. 11 (8) (2010) 751–758 (Epub 2010 Jul 11).

[28] M. Chen, M. Divangahi, H. Gan, D.S. Shin, S. Hong, D.M. Lee, C.N. Serhan, S.M. Behar, H.G. Remold, Lipid mediators in innate immunity against tuberculosis: opposing roles of PGE2 and LXA4 in the induction of macrophage death, J. Exp. Med. 205 (2008) 2791–2801.

[29] P. Prieto, J. Cuenca, P.G. Través, M. Fernández-Velasco, P. Martín-Sanz, L. Boscá, Lipoxin A4 impairment of apoptotic signaling in macrophages: implication of the PI3K/Akt and the ERK/Nrf-2 defense pathways, Cell Death Differ. 17 (7) (2010) 1179–1188 (Epub 2010 Jan 22).